



Antimicrobial activity of printed composite TiO₂/SiO₂ and TiO₂/SiO₂/Au thin films under UVA-LED and natural solar radiation

Irina Levchuk^{a,b,*}, Marcela Kralova^c, Juan José Rueda-Márquez^d, Javier Moreno-Andrés^b, Sergio Gutiérrez-Alfaro^b, Petr Dzik^c, Stephane Parola^e, Mika Sillanpää^d, Riku Vahala^a, Manuel A. Manzano^b

^a Water and Wastewater Engineering Research Group, School of Engineering, Aalto University, PO Box 15200, FI-00076 Aalto, Finland

^b Department of Environmental Technologies, INMAR-Marine Research Institute. Faculty of Marine and Environmental Sciences, Cadiz University, Polígono Rio San Pedro s/n, Puerto Real, 11510, Cadiz, Spain

^c Central European Institute of Technology, Brno University of Technology, Purkynova 648/125, 62100 Brno, Czech Republic

^d Laboratory of Green Chemistry, Lappeenranta University of Technology, Sammonkatu 12, 50130 Mikkeli, Finland

^e Laboratoire de Chimie, ENS Lyon, CNRS, Université Claude Bernard Lyon 1, Université de Lyon, UMR 5182, 46 allée d'Italie, 69364 Lyon, France

ARTICLE INFO

Keywords:

Escherichia coli
Total coliforms
Enterococci
Water disinfection
Gold bipyramids

ABSTRACT

Composite TiO₂/SiO₂ porous coatings modified with bipyramid-like gold nanoparticles were prepared by means of sol-gel and inkjet printing technique, comprehensively characterized and studied for photocatalytic disinfection of drinking water with fecal contamination by natural bacteria consortia. Photocatalytic antimicrobial activity of prepared thin films was evaluated against gram-negative (*Escherichia coli* and Total coliforms) and gram-positive bacteria (*Enterococci*). Elimination rate of all tested bacteria increased when photocatalytic coatings were used in comparison with solar disinfection. The best results in terms of antimicrobial activity were obtained with TiO₂/SiO₂/Au thin films under natural solar radiation, which demonstrated the highest antimicrobial activity, enhancing the inactivation rates of *E. coli*, Total coliforms and *Enterococci* 1.5, 1.3 and 1.6 times, respectively as compared to solar disinfection without photocatalyst. Remarkable difference in bacteria sensitivity for photocatalytic disinfection was observed with trend *E. coli* > Total coliforms > *Enterococci*. No release of gold and titanium was detected during photocatalytic water disinfection test. Regrowth of *E. coli*, Total coliforms and *Enterococci* after photocatalytic bacteria inactivation under UVA-LED and natural solar radiation was lower than 1% (24, 48 and 72 h), indicating potential application of prepared coatings for production of safe drinking water.

1. Introduction

Photocatalytic water treatment resulting in degradation of organic pollutants and pathogen's elimination has gained extensive attention in last decades as a promising option for the development of environmentally friendly technologies [1–3]. The most widely used photocatalyst is titanium dioxide in form of nanoparticles. The advantages of titanium dioxide include its chemical non-toxicity, relatively low cost and high photocatalytic activity [4–6]. Despite all advantages, this method has not found many practical applications in water treatment due to difficulties arising when nanoparticles should be separated from treated water.

Modification of TiO₂ with noble metals, such as silver and platinum, leads not only to the extension of photocatalytic activity towards visible

light but also to the increase of TiO₂ antimicrobial activity [7]. Thus, TiO₂ modified with Au were reported to be more efficient for inactivation of various bacteria than TiO₂ under radiation [8–10]. Interestingly, antimicrobial effects of TiO₂ modified with Au in darkness were also recently reported [11,12]. However, little is known regarding antimicrobial properties of TiO₂ modified with Au when prepared using inkjet printing (material printing) technique. Inkjet printing of sol-gel materials is novel approach and only few studies were reported so far on photocatalytic properties of printed semiconductors such as TiO₂ [13,14]. It is worth making a point that material printing of photocatalyst can be highly beneficial for scaling up.

To date majority of studies on photocatalytic water disinfection are conducted with pure cultures of bacteria added to distilled or synthetic water [15]. Only few works deal with photocatalytic inactivation of

* Corresponding author at: Water and Wastewater Engineering Research Group, School of Engineering, Aalto University, PO Box 15200, FI-00076 Aalto, Finland.
E-mail address: irina.levchuk@aalto.fi (I. Levchuk).

consortia of bacteria naturally present in real water [16–18] or synthetic water prepared in accordance with recommendations of WHO [19].

It is worth making a point that most commonly used source of radiation for photocatalytic water disinfection is different types of lamps [15], while the use of solar light is less common.

As far as we know, there are no studies on solar inactivation of natural fecal bacteria consortia in drinking water using printed $\text{TiO}_2/\text{SiO}_2$ and $\text{TiO}_2/\text{SiO}_2$ modified with gold nanoparticles. Hence, in this study $\text{TiO}_2/\text{SiO}_2$ and $\text{TiO}_2/\text{SiO}_2$ modified with gold nanoparticles in form of bipyramid were prepared by material printing technique. Moreover, feasibility of printed films for solar disinfection of drinking water contaminated with natural consortia of fecal bacteria for production of potable water was studied. Effect of film thickness, source of radiation (solar light and UVA-LEDs) as well as water matrix on antimicrobial properties of printed films was investigated.

2. Materials and methods

2.1. Preparation of $\text{TiO}_2/\text{SiO}_2/\text{Au}$ thin films

Hybrid silica sol was prepared according to procedure reported in earlier works [20–23]. Gold bipyramid-like nanoparticles were prepared following steps described below. 1200 μL of HAuCl_4 (25 mM in water) was mixed with 40 mL CTAB (47 mM in water). After that 1050 μL of aqueous silver nitrate (5 mM) was added, followed by 700 μL of 8-hydroxyquinoline (0.4 M in ethanol). Addition of silver ions was of high importance for controlled growth of Au bipyramids [24]. It was observed that growth solution became slightly yellowish. Then, 6–7 nm CTAC-capped gold seeds (4500 μL , 0.25 mM in Au^3) was added under stirring to the growth solution. After stirring for about 20 s, the growth solution stayed in the oven at 40–45 °C for 45 min. After cooling during an hour at ambient temperature, the solution was centrifuged at 8000 rpm for 30–60 min. The supernatant was replaced with CTAB solution (1 mM). After repeating this procedure one more time, nanoparticles were dispersed in half of the initial suspension volume of Milli-Q water. The concentration of gold bipyramid-like nanoparticles in final solution was about 0.3 g L^{-1} . More details concerning preparation of Au bipyramid-like nanoparticles can be found elsewhere [23,24].

In order to prepare hybrid $\text{TiO}_2/\text{SiO}_2/\text{Au}$ sol, 1 g of titanium dioxide nanoparticles were added to 50 mL of Milli-Q water under vigorous stirring and sonication. Obtained mixture was centrifuged at 10,000 rpm during 20 min. After removal of supernatant, ethanol (5 mL) and methyltriethoxysilane (MTEOS) sol (5 g, 20% wt.) were added. Final sol was sonicated. The $\text{TiO}_2/\text{SiO}_2$ sol was prepared in a similar way, but without addition of gold nanoparticles.

Thin films were deposited on borosilicate glass slides (Capitol Scientific) with size 2.5×7.5 cm. In order to remove dust and fat from the surface of glass slides, prior deposition, they were sonicated in aqueous solution of Neodisher detergent (BMT, Czech Republic), rinsed with water and dried in the airstream.

Since the solid content of originally prepared sols was too high for inject printing, the sols were diluted with isobutanol (50:50 v/v). After that, sols for printing were vigorously shaken with 1 mm glassballs overnight to break TiO_2 agglomerates. Experimental inkjet printer Fujifilm Dimatix 2831 was used for thin film deposition. The Digimax printhead with 16 nozzles was attached to the ink tank. The nozzle span and temperature were 30 μm and 30 °C, respectively. The glass slides were heated to 40 °C during printing. Films of $\text{TiO}_2/\text{SiO}_2$ and $\text{TiO}_2/\text{SiO}_2/\text{Au}$ were printed at five levels of film thickness (from one to five layers) in “wet-to-wet” manner (subsequent layer was printed on the top of the previous one without drying). After deposition, thin films were dried at 120 °C for 24 h. Prior to photocatalytic disinfection tests thin films were treated under UVC radiation (1.2 mW cm^{-2}) in water in order to remove residual organic molecules from the films.

2.2. Material characterization

The morphology of prepared thin films was examined with scanning electron microscope (SEM) Carl Zeiss Ultra Plus. The chemical composition of the samples was evaluated using energy dispersive X-ray spectroscopy (EDX, Oxford X-max with silicon drift detector) and X-ray photoelectron spectroscopy (XPS). The XPS measurements were conducted with Thermo Fisher Scientific ESCALAB 250Xi spectrometer under vacuum $\sim 10^{-7}$ mbar. Al K α radiation was used as X-ray source (1486.6 eV). For calibration of binding energy scale the positions of Ag 3d, Au 4f and Cu 2p peaks were measured. Crystallinity of printed films was examined by means of X-ray diffractometer Bruker D8ADVANCE-A25 Davinci TWIN-TWIN with Cu K α as the radiation source. The thickness of the films was determined with BRUKER DEKTAK XT profilometer. UV–vis spectrometer with integrating sphere was used to obtain optical characteristics of prepared thin films. The indirect band gaps of printed films were estimated from diffuse reflectance spectra (Agilent Cary 5000 UV–Vis-NIR double-beam spectrophotometer). Photoinduced hydrophilicity of prepared thin films was analysed by measuring contact angle of water droplets (volume 5 μL) on the surface of irradiated coatings. Radiation was provided by mercury lamp OSRAM HQL 125 W with intensity 10 mW cm^{-2} . After certain time intervals (10, 20, 30 and 60 min), three droplets were deposited on the irradiated surface of films and average value was taken. Measurements were performed with OCA20 contact angle meter. The hardness of all prepared thin films was tested through standard pencil hardness test [25]. Pencils with different hardness were successively placed into the pencil tester, from hardest to softest, and the hardness of pencil that will not cut into or gouge the film was evaluated as the hardness of the layer. The pencils were fixed in the tester firmly against the film at 45° angle and the speed of the tester was approximately 1 mm s^{-1} .

2.3. Tested water

As suggested by World Health Organization [19] various indicator microorganisms were obtained from real municipal wastewater by addition to drinking water. Thus, for photocatalytic disinfection experiments bottled drinking water (with relatively low concentration of salts) was inoculated with urban wastewater influent (1% v/v [19]), obtained from municipal wastewater treatment plant (WWTP) located in Chiclana de la Frontera, Cádiz (Spain). When effect of water matrix on bacteria inactivation was studied bottled water with relatively high concentration of salts was used and inoculated with urban wastewater in a similar way.

2.4. Photocatalytic disinfection tests

The UVA-LED based disinfection experiments were conducted in batch mode at room temperature 22 ± 2 °C. Thin films printed on borosilicate glass with total geometric area of 8 cm^2 were located in the reactor (glass Petri dish) with total volume of water 20 mL (the height of water level was 7.5 mm). The UVA-LED lamp (370 nm, an optical power density 22 mW cm^{-2}) was located above reactors (at distance 1 cm). All experiments were carried out under constant magnetic stirring. The UVA dose (using LEDs) was calculated by following equation:

$$D_{\text{UVA,LED}} = D_{t-1} + I_t \cdot \Delta t \quad (1)$$

where, I_t is the UVA radiation emitted by the LEDs (constant value of 220 W m^{-2}), Δt is the time between sampling (h).

Solar disinfection tests were performed in 600 mL borosilicate batch vessel reactors filled with 30 mL of water (the height of water level was 7.5 mm) and thin films (8 cm^2) under natural solar radiation at sunny day (with some clouds during first 30 min of test) around noon at University of Cádiz (36°31'43.6'' N - 6°12'49.0'' W). Reactors were

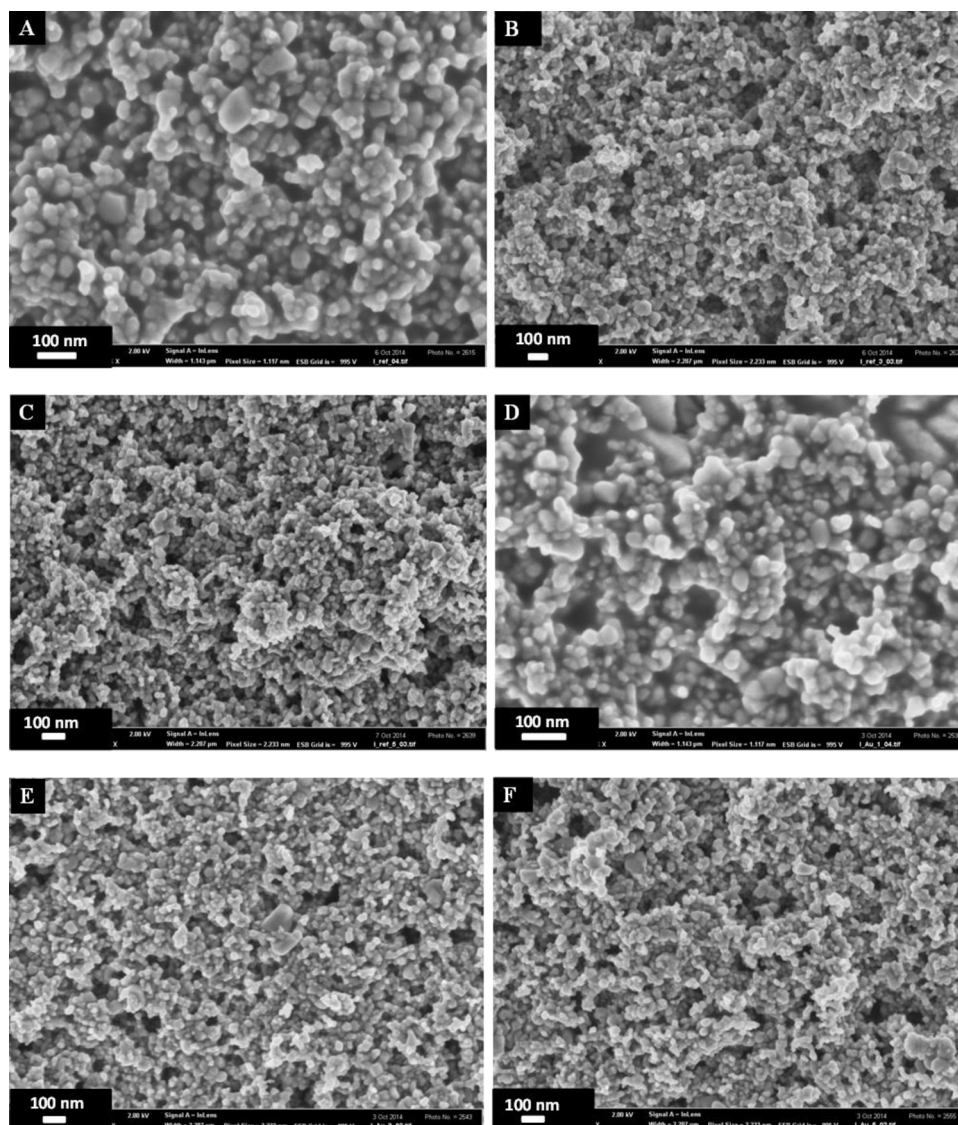


Fig. 1. Images from SEM analysis: A – TiO₂/SiO₂ one layers, B – TiO₂/SiO₂ three layers, C – TiO₂/SiO₂ five layers, D – TiO₂/SiO₂/Au one layers, E – TiO₂/SiO₂/Au three layers, F– TiO₂/SiO₂/Au five layers.

under constant magnetic stirring. UV radiation was measured by means of global UV radiometer CUV 5 (Kipp and Zonnen, the Netherlands). The results of solar water disinfection were represented as a function of cumulative UV dose (Q_{UV} , in Wh m^{-2}). The Q_{UV} was calculated according to the following equation:

$$Q_{UV,n} = Q_{UV,n-1} + \Sigma(UV_n \Delta t) \quad (2)$$

where $Q_{UV,n}$ is the cumulative UV dose received at each instant in Wh m^{-2} , UV_n is the irradiance of UV radiation recorded for each time interval in W m^{-2} , Δt is the time interval between radiation measurements (ten seconds) in hours.

Antimicrobial effect of different photocatalysts thin films was evaluated through fitting experimental points in traditional log-linear approach for describing microbial inactivation curves ($N = N_0 e^{-k \cdot UV \text{Dose}}$), as described elsewhere [26].

2.5. Reagents and analytical methods

The CTAB (cetyltrimethylammonium bromide, 99%), CTAC (25% cetyltrimethylammonium chloride solution in water), 2-methyl-8-hydroxyquinoline (MHQL, 98%) and 8-hydroxyquinoline (HQL, 99%) were purchased from Aldrich. Methyltriethoxysilane (MTEOS) was

received from ABCR, Tetrachloroauric acid trihydrate (99.9%) and silver nitrate were delivered by Alfa Aesar. Titanium dioxide (P25) with surface area $50 \text{ m}^2 \text{g}^{-1}$ was purchased from Degussa-Hüls-AG. The purification of the 8-hydroxyquinoline was performed using following steps: 1) dissolution in refluxing toluene, 2) hot filtration on a silica plug and crystallization.

Microbiological determination has been evaluated through colony counts on selective agar-based medium: Chromogenic Colinstant Agar (Scharlau) for Total coliforms and *Escherichia coli*; Slanetz-Barley Agar + TTC (1% v/v) (Panreac) for *Enterococci*.

Total coliform, *E. coli* and *Enterococci* were monitored by the membrane filtration method according to Standard Methods [27]. Ten-fold dilutions were filtrated through gridded membranes of $0.45 \mu\text{m}$ (Pall Corporation, NY, USA) and subsequently plated into Petri dishes with selective agar-based medium. Plates were incubated at 37°C for 24–48 h. The mean microbiological concentration of each sample was always with a variation coefficient of less than 30% as acceptance criteria. Results were expressed as colony forming units per milliliter of water (CFU mL^{-1}).

Various pathogenic bacteria have ability to show very low levels of metabolic activity during water treatment as well as ability to repair due to repair mechanisms [28] during storage and distribution of water

[29]. Hence, regrowth of *E. coli*, Total coliforms and *Enterococci* after photocatalytic disinfection was studied in order to check if applied treatment leads to destruction of bacteria or their temporary inactivation causing reactivation and regrowth after treatment. Regrowth experiments were conducted during 72 h, water samples after photocatalytic disinfection were stored in sterile containers in darkness at ambient temperature and 1 mL of sample was taken after each 24 h. Percentage of dark repair was calculated according to [30].

Concentration of anions in tested bottled water (prior addition of wastewater) was analysed using 881-Compact IC Pro (Metrohm) ion chromatograph (IC) equipped with ASupp5 250/4.0 column and conductivity detector. Cation concentrations were measured by means of 882-Compact IC Plus (Metrohm) IC using C4 250/4.0 column and conductivity detector. Mobile phase and flow rate for anion and cation analysis was mixture of CO_3^{2-} (3.20 mM), HCO_3^- (1 mM) at rate 0.7 mL min^{-1} and HNO_3 (1.7 mM), $\text{C}_7\text{H}_5\text{NO}_4$ (0.7 mM) at rate 0.9 mL min^{-1} , respectively. Water pH was measured using Crison GLP 21. Concentration of carbonates and bicarbonates present in water were measured with Titrand 905- Metrohm. Concentration of dissolved titanium and gold in water after disinfection tests was measured by means of inductively coupled plasma atomic emission spectrometry (ICP-AES) Thermo Iris Interpid.

3. Results and discussion

3.1. Characterization of printed $\text{TiO}_2/\text{SiO}_2$ and $\text{TiO}_2/\text{SiO}_2/\text{Au}$ thin films

SEM was applied to study and compare morphology of composite $\text{TiO}_2/\text{SiO}_2$ and $\text{TiO}_2/\text{SiO}_2/\text{Au}$ thin films. As shown in Fig. 1 all prepared coatings were porous with homogeneous microstructure. Morphology of prepared coatings was similar to those reported in preceding works [20,23]. The thickness of thin films was measured by profilometer.

The crystal phase of printed $\text{TiO}_2/\text{SiO}_2$ and $\text{TiO}_2/\text{SiO}_2/\text{Au}$ films was detected by means of X-ray diffraction patterns. Both anatase and rutile phase were present in unmodified and modified $\text{TiO}_2/\text{SiO}_2$ coatings (Fig. 2) as expected since TiO_2 (P25) was used during sol preparation and no further modification of crystallinity (such as annealing) was conducted. The presence of Au was not detected by XRD measurements, which can be possibly explained by low concentration of Au. Similar observations were reported earlier [31].

Chemical composition of composite thin films was evaluated by means of EDX and XPS (Figs. 3 and 4). The EDX measurements were performed before UV pretreatment of coatings. Hence, carbon levels are relatively high due to presence of organic compounds in the matrix of the film [20]. Presence of gold nanoparticles in modified $\text{TiO}_2/\text{SiO}_2$ thin films was confirmed by EDX measurements as shown in Fig. 3B. The typical XPS spectra of Ti 2p, O 1s, Si 2p, C 1s and Au 4f for $\text{TiO}_2/\text{SiO}_2/\text{Au}$ films are presented in Fig. 4. Presence of Au nanoparticles was

confirmed by detectable Au 4f signal (insert in Fig. 4). The Ti 2p peak indicated that titanium is present in Ti^{4+} state.

In order to confirm that the shape of gold nanoparticles was bi-pyramid-like, the reflectance measurements were conducted by means of UV-vis spectrometer with integrating sphere. From the Fig. 5 it is worthwhile to note presence of longitudinal SPR around 610 nm and transverse SPR band around 520 nm, which confirms presence of bi-pyramid-like Au nanoparticles in the matrix of $\text{TiO}_2/\text{SiO}_2$ film modified with gold as shown in our earlier study [23].

A widely applied method for band gap evaluation of semiconducting materials is graphing the square root of the Kubelka-Munk function multiplied by photon energy as a function of photon energy [32]. Extrapolation of linear part of obtained curve to zero is known as indirect band gap. The indirect band gaps of $\text{TiO}_2/\text{SiO}_2$ and $\text{TiO}_2/\text{SiO}_2/\text{Au}$ film were 2.98 and 2.88 eV, respectively. The decrease of indirect band gap with introduction of Au nanoparticles can be possibly explained by introduction of energy levels into band gap of $\text{TiO}_2/\text{SiO}_2$ film. Similar observations were reported for semiconductors modified with transition metals [31–33].

Measurements of water contact angle on the surface of $\text{TiO}_2/\text{SiO}_2$ and $\text{TiO}_2/\text{SiO}_2/\text{Au}$ thin films as a function of the UV illumination time were conducted in order to estimate hydrophilic properties of prepared coatings. Contact angles of freshly printed coatings varied between 100–120°. However, already after 10 min under UV light, the contact angle significantly decreased, confirming occurrence of photoinduced hydrophilicity (Fig. 6). Interestingly, transformation of surface from hydrophobic to hydrophilic under UV illumination was significantly faster for thin films modified with Au.

The hardness of prepared coatings was estimated in accordance with the standard test using the pencils in whole range of hardness. Printed thin films with various thicknesses were examined and no significant difference was observed. Maximum hardness (10 H) was attributed to all tested coatings except one layered $\text{TiO}_2/\text{SiO}_2$, which was slightly softer (2 H).

3.2. Photocatalytic water disinfection

3.2.1. Water characterization

Concentration of anions and cations in bottled drinking water (before addition of urban wastewater) was measured by means of Ion Chromatography. In soft drinking water concentrations of Na^+ , K^+ , Mg^{2+} , Ca^{2+} , Cl^- , NO_3^- , SO_4^{2-} , HCO_3^- were 4.23, 0.92, 0.66, 6.21, 4.69, 7.05, 3.98, 1 mg L^{-1} , respectively. In hard drinking water concentrations of Na^+ , K^+ , Mg^{2+} , Ca^{2+} , Cl^- , NO_3^- , SO_4^{2-} , HCO_3^- were 6.50, 0.59, 14.45, 83.08, 7.90, 10.05, 27.51, 203 mg L^{-1} , respectively. The pH of soft water was 7.3 and for hard water 7.7. The initial concentration of *Escherichia coli*, Total coliforms and *Enterococci* was about 10^2 CFU mL^{-1} , 10^2 – 10^3 CFU mL^{-1} and 10^2 CFU mL^{-1} , respectively in bottled drinking water after inoculation with municipal wastewater. The UV transmittance (280–400 nm) of drinking water inoculated with wastewater was higher than 95% (Fig. 7).

3.2.2. Effect of thin film thickness

As demonstrated in preceding works, the initial photocatalytic rates are proportional to the thickness of the $\text{TiO}_2/\text{SiO}_2$ thin films [34,35]. However, at certain limit the reaction rate becomes independent on film thickness. This limit mostly depends on applied operational conditions [36]. Therefore, it is of high importance to determine effect of film thickness of prepared photocatalytic coatings on inactivation of bacteria. As number of printed layers increased, so did the thickness of thin films (measured by means of surface profilometry). Thus, the thickness of 0.045, 0.063 and 1.235 μm was attributed to $\text{TiO}_2/\text{SiO}_2$ thin films of one, three and five layers, respectively. The thickness of $\text{TiO}_2/\text{SiO}_2/\text{Au}$ coatings with one, three and five layers was 0.459, 1.190 and 1.414 μm , respectively. Preliminary UVA-LED disinfection runs were performed examining the effect of $\text{TiO}_2/\text{SiO}_2$ and $\text{TiO}_2/\text{SiO}_2/\text{Au}$

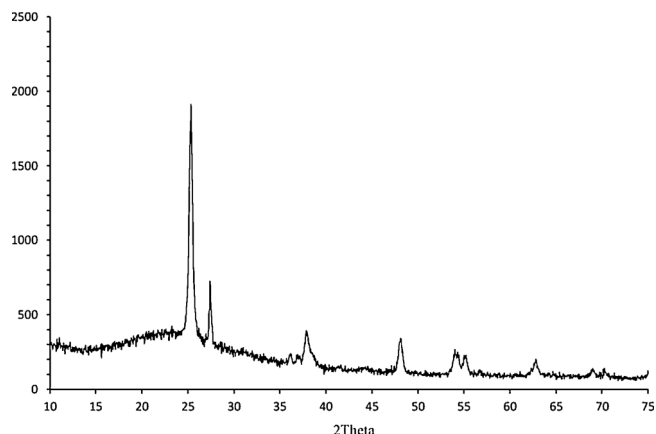


Fig. 2. Typical XRD spectra for $\text{TiO}_2/\text{SiO}_2/\text{Au}$ films.

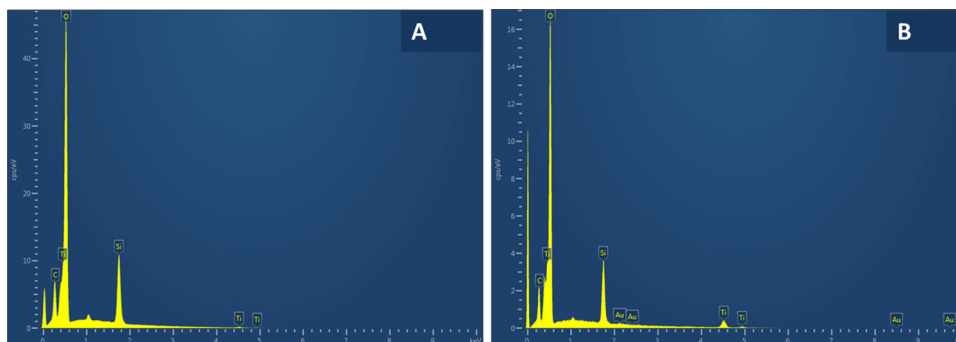


Fig. 3. Chemical composition of thin films: A – TiO₂/SiO₂ (5 layers), B – TiO₂/SiO₂/Au (5 layers).

film thickness on inactivation of Total coliforms. The Total coliforms were chosen because of higher initial concentration among all tested microorganisms obtained from natural bacteria consortia. Enhancement of bacteria inactivation was observed for the illuminated TiO₂/SiO₂ and TiO₂/SiO₂/Au coatings (5 layers) in comparison with photolysis, indicating evident antimicrobial capacity of printed films. According to the results obtained through Log-linear modeling (Table 1), an increase of kinetic rate constant (k_{\max} , $\text{m}^2\text{W}^{-1}\text{h}^{-1}$) by 113% (5 Layers) determine the higher inactivation efficiency of the TiO₂/SiO₂ and TiO₂/SiO₂/Au photocatalytic film as compared to photolysis (Fig. 8).

It is difficult to speculate the role of Au nanoparticles in enhancement of disinfection rate, other than to note that thickness, and as a result TiO₂ loading, was different for TiO₂/SiO₂ and TiO₂/SiO₂/Au films except coatings with five layers. Hence, all sequential photocatalytic disinfection tests were conducted using five layered TiO₂/SiO₂ and TiO₂/SiO₂/Au. To our knowledge, only one study on photocatalytic water disinfection using TiO₂/SiO₂ thin films has been reported [37]. In former study higher inactivation rate of *E. coli* was achieved in the range of film thickness (about 1 μm) similar to our work (TiO₂/SiO₂ and TiO₂/SiO₂/Au with five layers) [37].

3.2.3. Antimicrobial activity for different types of bacteria

Antimicrobial activity was compared for three typical indicators that normally appear in drinking water with fecal contamination *E. coli*, Total coliforms and *Enterococci* (Fig. 9). In this case, photocatalytic coatings with optimal thickness (five layers) were selected for evaluation of different factors such as the sensitivity of various microorganisms. The sensitivity followed the trend: *E. coli* > Total coliforms > *Enterococci*. Similar results have been reported elsewhere [38–41]. A

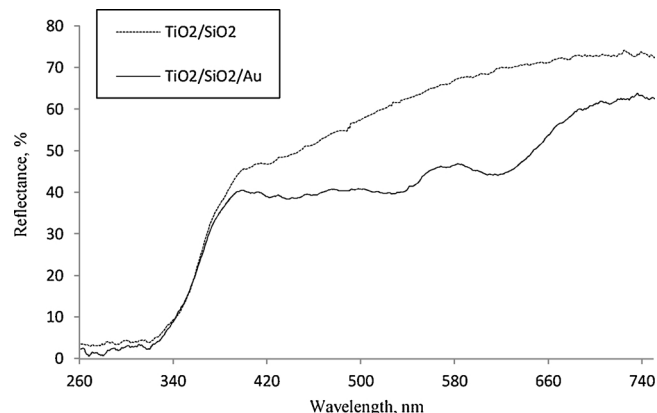


Fig. 5. Reflectance spectra of TiO₂/SiO₂ (5 layers) and TiO₂/SiO₂/Au (5 layers) thin films.

plausible reason for variations in tested bacteria response could be related to the differences in the cell wall structure.

Gram-negative bacteria, such as *E. coli* and Total coliforms have a complex structure given by the outer membrane, in which two lipid bilayers may present the major $\cdot\text{OH}$ target for photocatalytic processes [41]. An improvement of disinfection rate towards tested gram-negative bacteria with TiO₂/SiO₂ and TiO₂/SiO₂/Au was clearly observed as compared to UVA photolysis. Thus, complete inactivation of Total coliforms was achieved using TiO₂/SiO₂/Au ($165 \text{ W}\cdot\text{h m}^{-2}$), while even at maximum experimental dose ($220 \text{ W}\cdot\text{h m}^{-2}$) full inactivation was not reached during photolysis and application of TiO₂/SiO₂. More conclusive results were obtained for *E. coli*. The dose required for achieving

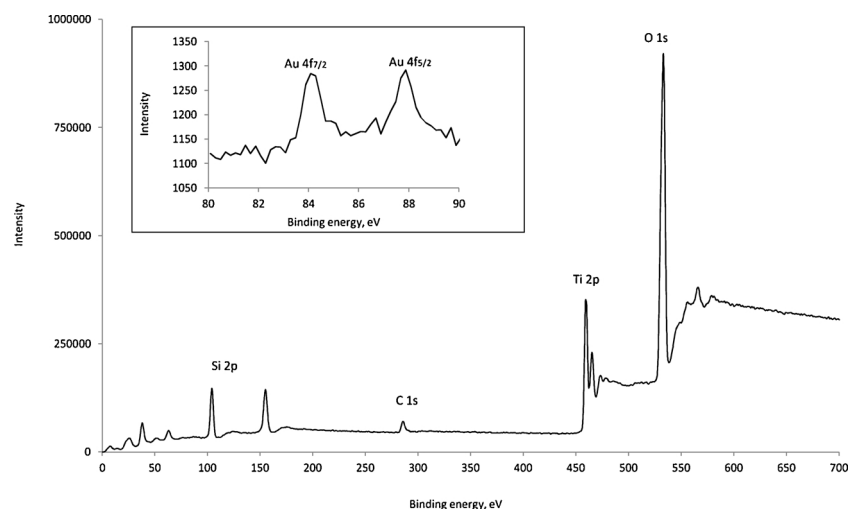


Fig. 4. Typical XPS spectrum of TiO₂/SiO₂/Au film; Insert: Typical XPS spectrum of the Au4f levels of TiO₂/SiO₂/Au film.

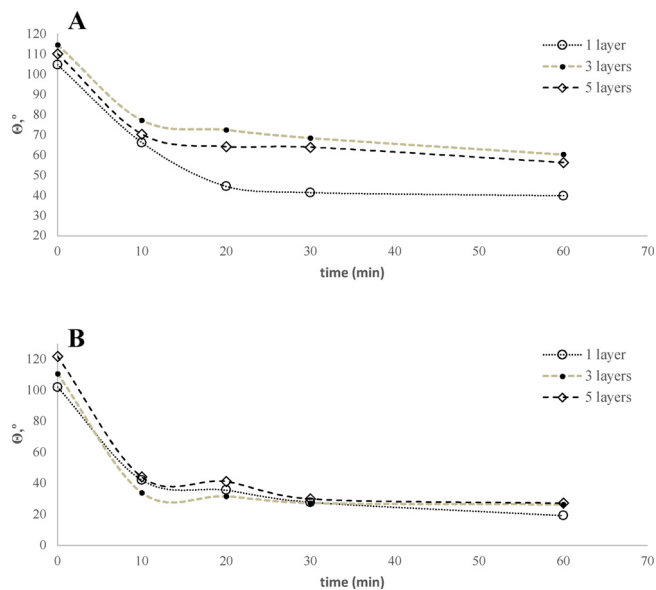


Fig. 6. Water contact angle of $\text{TiO}_2/\text{SiO}_2$ thin films (A) and $\text{TiO}_2/\text{SiO}_2/\text{Au}$ thin films (B) as a function of UV illumination time.

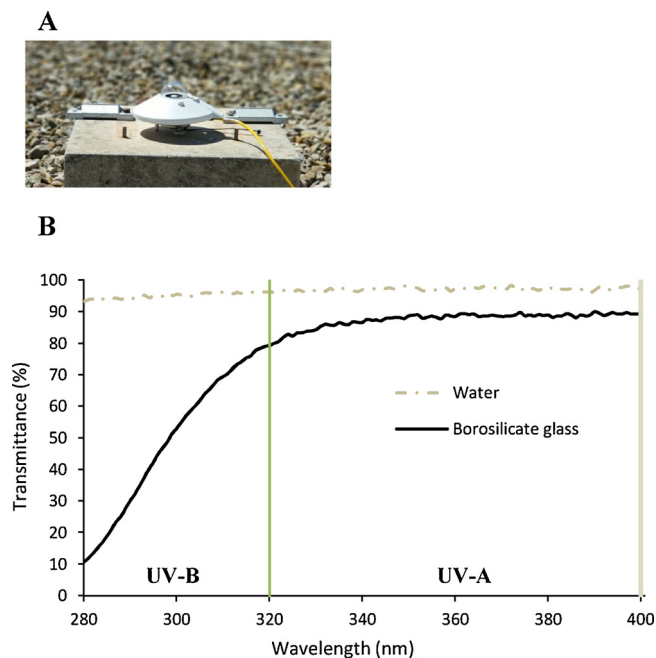


Fig. 7. A) radiometer B) transmittance of tested water and borosilicate glass from 280 to 400 nm.

detection limit of *E. coli* was $165 \text{ W}\cdot\text{h m}^{-2}$ and $110 \text{ W}\cdot\text{h m}^{-2}$ when $\text{TiO}_2/\text{SiO}_2$ and $\text{TiO}_2/\text{SiO}_2/\text{Au}$ were applied, respectively. An increase of k_{\max} for $\text{TiO}_2/\text{SiO}_2/\text{Au}$ was estimated to be 87.5% as compared to $\text{TiO}_2/\text{SiO}_2$.

Enterococci was the most resistant group in all systems, both photocatalytic and photocatalytic. As gram-positive bacteria, it has a thicker wall, mainly constituted of a porous peptidoglycan layer. Some authors suggested that gram-positive bacteria can gain an advantage in survival when oxidant species are attacking the cell wall due to the thicker cell wall layer [40]. The difference of *Enterococci* inactivation rate using $\text{TiO}_2/\text{SiO}_2$ ($k_{\max} = 0.015 \text{ m}^2\text{W}^{-1}\text{h}^{-1}$) and $\text{TiO}_2/\text{SiO}_2/\text{Au}$ ($k_{\max} = 0.011 \text{ m}^2\text{W}^{-1}\text{h}^{-1}$) thin films was insignificant.

3.2.4. Effect of water matrix

Effect of water matrix on antimicrobial activity of prepared thin films was studied using soft and hard bottled water.

The effect of water matrix on inactivation of *E. coli* and Total coliforms is shown in Fig. 10. Significant inhibition of *E. coli* inactivation rate by photocatalytic films was observed when tests were conducted in hard water (Fig. 10A). Thus, complete elimination of *E. coli* when $\text{TiO}_2/\text{SiO}_2$ and $\text{TiO}_2/\text{SiO}_2/\text{Au}$ were used in soft water was achieved at UVA dose of about $165 \text{ W}\cdot\text{h m}^{-2}$ and $110 \text{ W}\cdot\text{h m}^{-2}$, respectively, whereas in contrast in hard water complete inactivation was not reached even after $220 \text{ W}\cdot\text{h m}^{-2}$. For $\text{TiO}_2/\text{SiO}_2$ *E. coli* inactivation rate in hard water was about 68.4% lower than that in soft water, while for $\text{TiO}_2/\text{SiO}_2/\text{Au}$ this value was about 63.4%. Interestingly, in case of Total coliforms inactivation rate inhibition in hard water was lower than in case of *E. coli*. Decrease of Total coliforms inactivation rate in hard water for $\text{TiO}_2/\text{SiO}_2$ was about 50%, while for $\text{TiO}_2/\text{SiO}_2/\text{Au}$ it was only 25%.

According to some studies [42] anions present in water can be adsorbed on the positively charged surface of TiO_2 , which may cause suppressive action on generation of hydroxyl radicals. Significant decrease of *E. coli* and Total coliforms elimination rate in hard water can be attributed to higher concentration of bicarbonates (203 mg L^{-1}), which can act as scavengers of hydroxyl radicals according to reaction (3) [43,44]. Inhibition of TiO_2 photocatalytic activity in presence of similar concentration of bicarbonates in water was reported [45].



3.2.5. Solar inactivation of *E. coli*, Total coliforms and *Enterococci*

The disinfection experiments under natural solar light were conducted in absence (SODIS) and presence of $\text{TiO}_2/\text{SiO}_2$ and $\text{TiO}_2/\text{SiO}_2/\text{Au}$. The mortality (in log scale) of *E. coli*, Total coliforms and *Enterococci* as a function of UV dose (from 280 to 400 nm) is shown in Fig. 11. From the Fig. 11 it is worthwhile to note that the elimination rate of all tested bacteria increased when photocatalytic coatings were used in comparison with SODIS. Interestingly, a shoulder can be observed in the beginning of SODIS process (first 30 min) for all tested microorganisms, which can be attributed to presence of clouds during first 30 min of solar test. This effect was not observed during the photocatalytic solar disinfection, suggesting that prepared photocatalytic thin films can be efficient even if solar irradiance is not optimal.

As noticed in previous experiments, *E. coli* was the most sensitive among tested microorganisms. The difference of *E. coli* inactivation rate with $\text{TiO}_2/\text{SiO}_2$ and $\text{TiO}_2/\text{SiO}_2/\text{Au}$ appears to be negligible (Table 2). Kinetic rate constants for $\text{TiO}_2/\text{SiO}_2$ and $\text{TiO}_2/\text{SiO}_2/\text{Au}$ were estimated to be $0.146 \text{ W}^{-1}\text{h}^{-1}\text{m}^2$ and $0.142 \text{ W}^{-1}\text{h}^{-1}\text{m}^2$, respectively. The UV dose required for complete inactivation of *E. coli* from water applying SODIS and photocatalytic disinfection was $55 \text{ W}\cdot\text{h m}^{-2}$ ($k_{\max} = 0.098 \text{ W}^{-1}\text{h}^{-1}\text{m}^2$) and $34 \text{ W}\cdot\text{h m}^{-2}$, respectively.

The $\text{TiO}_2/\text{SiO}_2/\text{Au}$ performed similar to $\text{TiO}_2/\text{SiO}_2$ and faster than SODIS for Total coliforms elimination, each attaining inactivation rate constant of 0.141, 0.138 and $0.106 \text{ W}^{-1}\text{h}^{-1}\text{m}^2$, respectively. In case of Total coliforms the UV dose required for complete inactivation was $76 \text{ W}\cdot\text{h m}^{-2}$ for SODIS and $55 \text{ W}\cdot\text{h m}^{-2}$ for photocatalytic disinfection. No significant difference was observed between $\text{TiO}_2/\text{SiO}_2$ and $\text{TiO}_2/\text{SiO}_2/\text{Au}$ for inactivation of *E. coli* and Total coliforms.

The kinetic rate constants for *Enterococci* inactivation using $\text{TiO}_2/\text{SiO}_2/\text{Au}$, $\text{TiO}_2/\text{SiO}_2$ and SODIS were 0.121, 0.077 and $0.073 \text{ W}^{-1}\text{h}^{-1}\text{m}^2$, respectively. The $\text{TiO}_2/\text{SiO}_2/\text{Au}$ film was more efficient than $\text{TiO}_2/\text{SiO}_2$ and SODIS, each attaining complete *Enterococci* elimination at UV dose of 34, 55 and $55 \text{ W}\cdot\text{h m}^{-2}$, respectively. This fact can be possibly explained by large solar spectra (UVB and UVA). *Enterococci* appear to be more resistant than *E. coli* and Total coliforms under natural solar radiation. In terms of kinetic inactivation rate the $\text{TiO}_2/\text{SiO}_2/\text{Au}$ was about 1.6 times (63.6%) more efficient than $\text{TiO}_2/\text{SiO}_2$ for *Enterococci* inactivation. It should be noted that such difference in photocatalytic antimicrobial activity of $\text{TiO}_2/\text{SiO}_2/\text{Au}$ towards

Table 1

Kinetic rate constants and statistical parameters obtained by fitting of experimental data in Log-linear model. Parameters were obtained for different treatments and layers (Organism: *T. coliforms*), organisms.

OPTIMIZATION PHASE					
Treatment		k_{\max} ($\text{m}^2 \text{Wh}^{-1}$) \pm S.E.	k_{\max} (min^{-1}) \pm S.E.	R^2	RMSE
UVA-LED		0.016 ± 0.001	0.058 ± 0.005	0.960	0.121
$\text{TiO}_2/\text{SiO}_2$	1 Layer	0.023 ± 0.003	0.083 ± 0.013	0.893	0.289
	3 Layers	0.022 ± 0.003	0.082 ± 0.009	0.931	0.228
	5 Layers	0.032 ± 0.004	0.117 ± 0.016	0.928	0.261
$\text{TiO}_2/\text{SiO}_2/\text{Au}$	1 Layer	0.020 ± 0.002	0.072 ± 0.005	0.971	0.127
	3 Layers	0.025 ± 0.003	0.091 ± 0.009	0.944	0.224
	5 Layers	0.032 ± 0.001	0.116 ± 0.004	0.996	0.062

Enterococci was not observed when UVA-LED was used as radiation source.

Solar spectra include UVA and UVB radiation. It is well known that damage for microorganisms by UVB is about 100–1000 times higher than by UVA [46], thus, being more harmful for all studied bacteria. This fact was confirmed by higher *E. coli* inactivation rate (about 4.4 times) during SODIS as compared to UVA-LED photolysis. Similar enhancement of disinfection rate was observed for *Enterococci*. These results are in agreement with preceding work [26]. Therefore, more sensitive bacteria such as *E. coli* and Total coliforms can be significantly affected by UVB radiation, which in turn does not permit to distinguish differences between $\text{TiO}_2/\text{SiO}_2$ and $\text{TiO}_2/\text{SiO}_2/\text{Au}$ photocatalytic thin films. However, for more resistant microorganism (*Enterococci*) significant difference between both materials was observed under solar radiation.

The damage produced during photocatalytic inactivation of tested bacteria by $\text{TiO}_2/\text{SiO}_2/\text{Au}$ films was investigated by means of SEM. The morphology changes of *E. coli*, Total coliforms and *Enterococci* observed before and during photocatalytic water disinfection are presented in Fig. 12. As shown in Fig. 12A all tested bacteria were present on the surface of photocatalyst prior solar water disinfection. The morphology of bacteria before photocatalytic disinfection was smooth and undamaged (Fig. 12B). At dose about 20 Wh m^{-2} the cells became cataplastic (Fig. 12C,D), suggesting significant damage of bacteria during photocatalytic solar disinfection.

3.2.6. Bacteria regrowth

It is well known that even after disinfection there is a possibility of bacteria regrowth. Therefore, it is of high importance to study survivability of bacteria after applied treatment. By the virtue of the fact that life time of highly reactive oxidizing species generated during photocatalytic water disinfection is short, inhibition of bacteria regrowth after treatment, like in case of chlorination, is not possible. In order to check possible bacteria regrowth during storage and distribution of

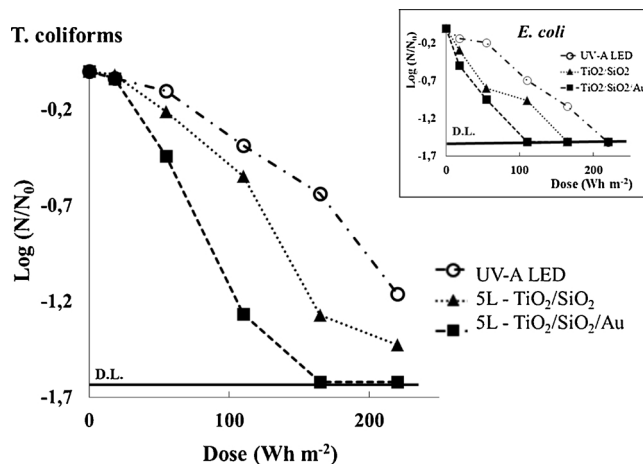


Fig. 9. Inactivation profiles obtained for Total coliforms and *E. coli* under UV-A LED radiation and photocatalytic treatment: $\text{TiO}_2/\text{SiO}_2$ 5 layers thin films and $\text{TiO}_2/\text{SiO}_2/\text{Au}$ 5 layers thin films. D.L. represents the detection limit.

photocatalytically treated drinking water, regrowth tests should be performed. Therefore, the regrowth of *E. coli*, Total coliforms and *Enterococci* after photocatalytic disinfection under UVA-LED and natural solar light as well as SODIS and photolysis was tested. When complete inactivation of microorganisms was reached water samples were poured into sterile containers and stored in dark place during 72 h. Regrowth was checked after 24 h, 48 h and 72 h for all samples. After UVA photolysis and SODIS the regrowth of all tested bacteria was below 5%, while after photocatalytic disinfection under UVA and solar light the value was below 1%. These results together with enhanced bacteria inactivation rate observed when printed photocatalytic films were used, suggest that $\text{TiO}_2/\text{SiO}_2$ and $\text{TiO}_2/\text{SiO}_2/\text{Au}$ are promising for drinking water disinfection.

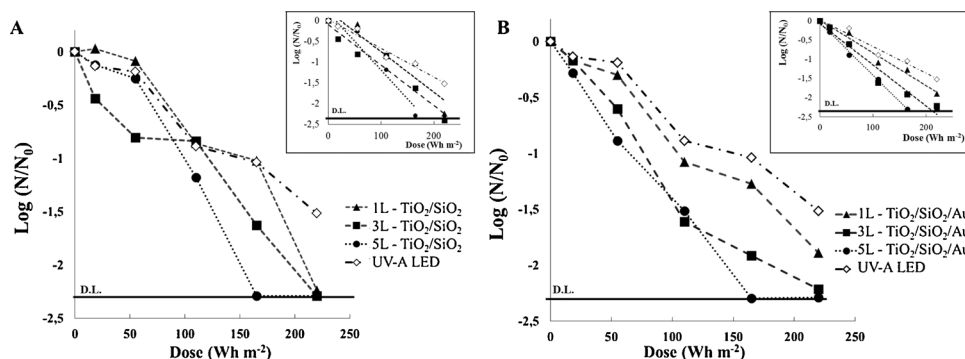


Fig. 8. Total coliforms inactivation under UVA-LED radiation at several layers of $\text{TiO}_2/\text{SiO}_2$ thin films (A) and $\text{TiO}_2/\text{SiO}_2/\text{Au}$ thin films (B). Inset shows the Log-linear modeling of experimental points. D.L. represents the detection limit.

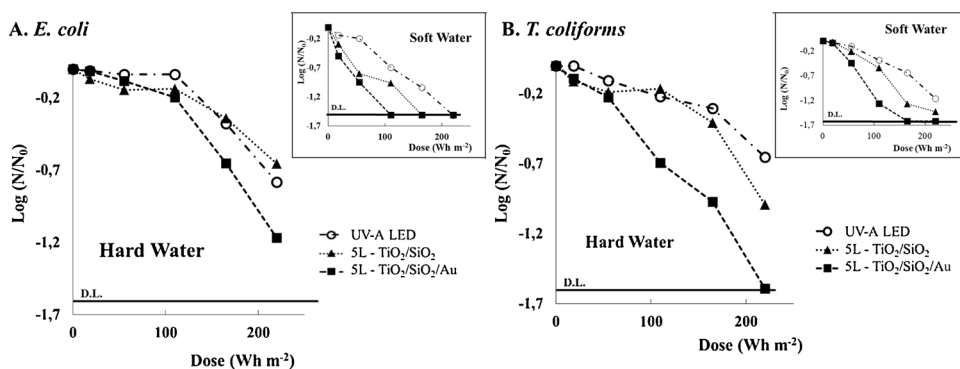


Fig. 10. Inactivation profiles obtained in hard water ($[\text{HCO}_3^{2-}] = 203 \text{ mg L}^{-1}$) for *E. coli* (A) and *T. coliforms* (B) under UV-A LED irradiation and photocatalytic treatment: $\text{TiO}_2/\text{SiO}_2$ 5 layers thin films and $\text{TiO}_2/\text{SiO}_2/\text{Au}$ 5 layers thin films. Inset shows the inactivation profiles in soft water ($[\text{HCO}_3^{2-}] = 1 \text{ mg L}^{-1}$). D.L. represents the detection limit.

3.2.7. Why modification with Au bipyramid-like nanoparticles enhance antimicrobial properties of $\text{TiO}_2/\text{SiO}_2$?

As it was reported in the literature, an increase of photocatalytic decomposition of organic pollutants by TiO_2/Au does not necessarily cause an improvement of its antimicrobial properties [47] and vice versa [8]. The $\text{TiO}_2/\text{SiO}_2/\text{Au}$ thin films prepared in this work were more efficient than $\text{TiO}_2/\text{SiO}_2$ under UVA and solar radiation for inactivation of *E. coli*, Total coliforms and *Enterococci* and for decomposition of formic acid, as reported in our earlier study [23]. Possible reasons for improvement of antimicrobial properties of $\text{TiO}_2/\text{SiO}_2/\text{Au}$ thin films prepared in this work can be: (i) enhanced photocatalytic activity [23] and/or (ii) biocidal nature of the Au. That is to say that when photocatalytic materials modified with metal are used, the increased disinfection performance may occur due to toxic effect of metal released to the solution (ii). Even very low concentrations of released metal can significantly affect the deactivation of bacteria due to oligodynamic effect [48]. According to recent study [49], presence of Au^+ and Au^{3+} ions in aqueous solution can significantly inhibit growth of various bacteria; for instance, IC_{50} for *E. coli* was achieved at $74.9 \mu\text{g L}^{-1}$ of Au^+ and $66.9 \mu\text{g L}^{-1}$ of Au^{3+} . Therefore, possible release of titanium and gold from prepared photocatalytic thin films was tested by measuring concentration in the water after disinfection. Concentration of titanium and gold in the treated water was below the detection limit ($2 \mu\text{g L}^{-1}$). In order to evaluate possible toxic effect of prepared thin films on *E. coli*, Total coliforms and *Enterococci* experiments were conducted in dark with $\text{TiO}_2/\text{SiO}_2$ and $\text{TiO}_2/\text{SiO}_2/\text{Au}$ thin films (5 layers). For this purpose, coatings were in contact with tested water during one hour in absence of radiation source. Inactivation of *E. coli*, Total coliforms and *Enterococci* did not occur during this period, suggesting absence of short-term toxicity to tested microorganisms during exposure to $\text{TiO}_2/\text{SiO}_2$ and $\text{TiO}_2/\text{SiO}_2/\text{Au}$. The concentration of titanium and gold in water after dark test was also measured and it was below the detection limit. Therefore, enhanced antimicrobial properties of $\text{TiO}_2/\text{SiO}_2/\text{Au}$ can be ascribed to improved photocatalytic activity. Enhanced

Table 2

Kinetic rate constants and statistical parameters obtained by fitting of experimental data in Log-linear model.

SOLAR TEST				
Treatment		$k_{\text{max}} (\text{m}^2 \text{Wh}^{-1}) \pm \text{S.E.}$	R^2	RMSE
SOLAR DISINFECTION (SODIS)	<i>T. coliforms</i>	0.106 ± 0.010	0.9583	0.2765
	<i>E. coli</i>	0.098 ± 0.007	0.9822	0.1233
	<i>Enterococci</i>	0.073 ± 0.015	0.8521	0.2826
$\text{TiO}_2/\text{SiO}_2$	<i>T. coliforms</i>	0.138 ± 0.014	0.9569	0.2747
	<i>E. coli</i>	0.146 ± 0.003	0.9983	0.0386
	<i>Enterococci</i>	0.077 ± 0.002	0.9974	0.0420
$\text{TiO}_2/\text{SiO}_2/\text{Au}$	<i>T. coliforms</i>	0.141 ± 0.022	0.9052	0.4224
	<i>E. coli</i>	0.142 ± 0.010	0.9833	0.1178
	<i>Enterococci</i>	0.121 ± 0.017	0.9413	0.1919

photocatalytic activity of composite films modified with Au NPs can possibly be explained by generation of highly reactive "hot" electrons by light excitation of Au NPs plasmon and electron transfer into TiO_2 [10,50].

4. Conclusions

This study focused on photocatalytic disinfection of drinking water with fecal contamination using printed $\text{TiO}_2/\text{SiO}_2$ and $\text{TiO}_2/\text{SiO}_2/\text{Au}$ thin films modified with bipyramid-like gold nanoparticles under UVA-LED and natural solar radiation. Photocatalytic antimicrobial activity of printed thin films was investigated against *E. coli*, Total coliforms and *Enterococci*. Key findings of this work are listed below.

- Antimicrobial activity of printed coatings improved with increase of thin film thickness (under UVA-LED radiation). The highest enhancement of inactivation rate was observed for $\text{TiO}_2/\text{SiO}_2$ and

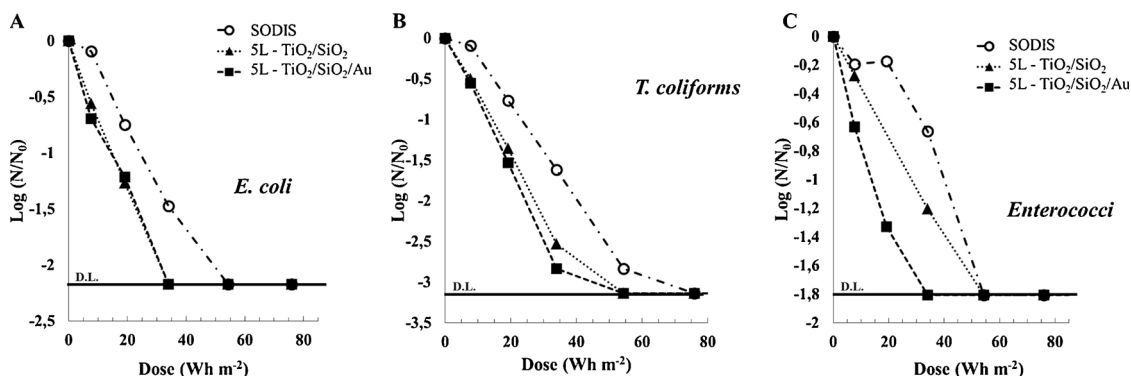


Fig. 11. Inactivation profiles obtained in Solar Test (SODIS) for *E. coli* (A), *T. coliforms* (B) and *Enterococci* (C) under solar radiation and photocatalytic treatment: $\text{TiO}_2/\text{SiO}_2$ 5 layers' thin films and $\text{TiO}_2/\text{SiO}_2/\text{Au}$ 5 layers' thin films. D.L. represents the detection limit.

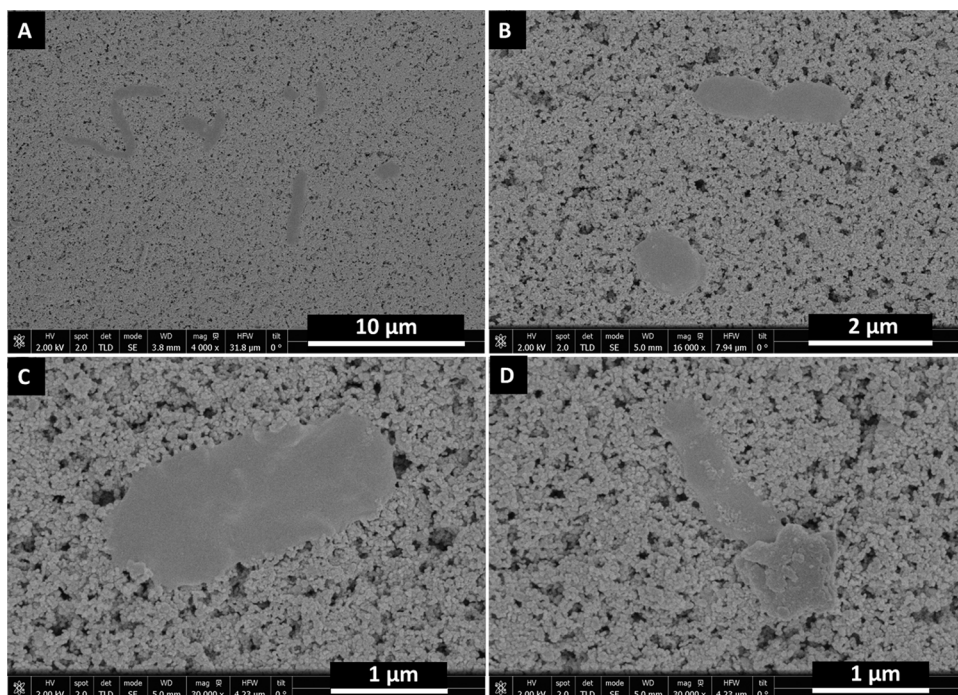


Fig. 12. SEM images of bacteria on the surface of $\text{TiO}_2/\text{SiO}_2/\text{Au}$ film with five layers at different time of solar photocatalytic disinfection: A – *E. coli*, Total coliforms and *Enterococci* on the surface at 0 Wh m^{-2} ; B – *E. coli* and *Enterococci* at 0 Wh m^{-2} ; C – residue of *E. coli* at 20 Wh m^{-2} ; D – residue of *E. coli* and *Enterococci* at 20 Wh m^{-2} .

$\text{TiO}_2/\text{SiO}_2/\text{Au}$ films, both leading to improvement of 113% (5 layers) for Total coliforms as compared to photolysis.

- Sensitivity of bacteria to photocatalytic water disinfection varied. Thus, *E. coli* was the most sensitive among all studied bacteria, while *Enterococci* was the most resistant.
- Significant effect of water matrix on photocatalytic water disinfection was observed. Inactivation rates drastically decreased when experiments were conducted in hard water with photocatalytic coatings.
- Based on conducted experiments it can be concluded that photocatalytic water disinfection using natural solar radiation is more efficient than high intensity UVA-LED radiation.
- Under natural solar radiation $\text{TiO}_2/\text{SiO}_2$ and $\text{TiO}_2/\text{SiO}_2/\text{Au}$ demonstrated similar disinfection for more sensitive bacteria (gram-negative). However, for more efficient inactivation of resistant bacteria (gram-positive) $\text{TiO}_2/\text{SiO}_2/\text{Au}$ was required.
- Lower level of bacteria regrowth was observed when photocatalytic materials were used ($< 1\%$) in comparison with photolysis and SODIS ($< 5\%$).
- No release of titanium and gold was detected during disinfection tests, suggesting that printed thin films are stable and suitable for practical applications.

Generally, based on results obtained in this study it can be concluded that printed $\text{TiO}_2/\text{SiO}_2$ and $\text{TiO}_2/\text{SiO}_2/\text{Au}$ coatings are promising for the elimination of pathogens from contaminated drinking water under natural solar radiation.

Acknowledgements

This Special Issue is dedicated to honor the retirement of Dr. John Kiwi at the Swiss Federal Institute of Technology (Lausanne), a key figure in the topic of photocatalytic materials for the degradation of contaminants of environmental concern. Authors would like to express gratitude to Professors Eduardo Blanco and Almudena Aguinaco Martin for help with band gap measurements.

References

- [1] L. Prieto-Rodriguez, S. Miralles-Cuevas, I. Oller, P. Fernández-Ibáñez, A. Agüera, J. Blanco, S. Malato, Appl. Catal. B 128 (2012) 119–125, <https://doi.org/10.1016/j.apcatb.2012.03.034>.
- [2] S. Malato, M.I. Maldonado, P. Fernández-Ibáñez, I. Oller, I. Polo, R. Sánchez-Moreno, Mater. Sci. Semicond. Process. 42 (2016) 15–23, <https://doi.org/10.1016/j.mssp.2015.07.017>.
- [3] R. Fagan, D.E. McCormack, D.D. Dionysiou, S.C. Pillai, Mater. Sci. Semicond. Process. 42 (2016) 2–14, <https://doi.org/10.1016/j.mssp.2015.07.052>.
- [4] O. Carp, C.L. Huisman, A. Reller, Prog. Solid State Chem. 32 (2004) 33–177, <https://doi.org/10.1016/j.progsolidstchem.2004.08.001>.
- [5] K. Eufinger, D. Poelman, H. Poelman, R. De Gryse, G.B. Marin, S.C. Nam (Ed.), Thin Solid Films: Process and Applications, 2008, pp. 189–227.
- [6] A. Fujishima, T.N. Rao, D.A. Tryk, J. Photochem. Photobiol. C Photochem. Rev. 1 (2000) 1–21, [https://doi.org/10.1016/S1389-5567\(00\)00002-2](https://doi.org/10.1016/S1389-5567(00)00002-2).
- [7] S. Sreeja, V. Shetty K, Sol. Energy 157 (2017) 236–243, <https://doi.org/10.1016/j.solener.2017.07.057>.
- [8] J.Š. Ogorevc, E. Tratar-Pirc, L. Matoh, B. Peter, Acta Chim. Slov. (2012) 264–272.
- [9] L. Guo, C. Shan, J. Liang, J. Ni, M. Tong, Colloids Surf. B Biointerfaces 128 (2015) 211–218, <https://doi.org/10.1016/j.colsurf.2015.01.013>.
- [10] J. Zhang, X. Suo, J. Zhang, B. Han, P. Li, Y. Xue, H. Shi, Mater. Lett. 162 (2016) 235–237, <https://doi.org/10.1016/j.matlet.2015.09.136>.
- [11] G. Wang, H. Feng, A. Gao, Q. Hao, W. Jin, X. Peng, W. Li, G. Wu, P.K. Chu, ACS Appl. Mater. Interfaces 8 (2016) 24509–24516, <https://doi.org/10.1021/acsami.6b10052>.
- [12] G. Wang, H. Feng, W. Jin, A. Gao, X. Peng, W. Li, H. Wu, Z. Li, P.K. Chu, Appl. Surf. Sci. 414 (2017) 230–237, <https://doi.org/10.1016/j.apsusc.2017.04.053>.
- [13] M. Černá, M. Veselý, P. Dzik, C. Guillard, E. Puzenat, M. Lepičová, Appl. Catal. B 138–139 (2013) 84–94, <https://doi.org/10.1016/j.apcatb.2013.02.035>.
- [14] M. Raimondo, G. Guarini, C. Zanelli, F. Marani, L. Fossa, M. Dondi, Ceram. Int. 38 (2012) 4685–4693, <https://doi.org/10.1016/j.ceramint.2012.02.051>.
- [15] J. Blanco-Galvez, P. Fernández-Ibáñez, S. Malato-Rodríguez, J. Sol. Energy Eng. 129 (1) (2006) 4–15.
- [16] R. Dillert, U. Siemon, D. Bahnemann, Chem. Eng. Technol. 21 (1998) 356–358.
- [17] J.H. Melián, J.D. Rodríguez, A.V. Suárez, E.T. Rendón, C.V. Do Campo, J. Arana, J.P. Peña, Chemosphere 41 (2000) 323–327.
- [18] A. Rincón, C. Pulgarin, Appl. Catal. B 49 (2004) 99–112, <https://doi.org/10.1016/j.apcatb.2003.11.013>.
- [19] World Health Organization (2011).
- [20] D. Gregori, I. Benchenaa, F. Chaput, S. Therias, J. Gardette, D. Léonard, C. Guillard, S. Parola, J. Mater. Chem. A 2 (2014) 20096–20104.
- [21] D. Chateau, F. Chaput, C. Lopes, M. Lindgren, C. Brännlund, J. Öhgren, N. Djourelou, P. Nedelec, C. Desroches, B. Eliasson, T. Kindahl, F. Lerouge, C. Andraud, S. Parola, ACS Appl. Mater. Interfaces 4 (2012) 2369–2377.
- [22] D. Chateau, Q. Bellier, F. Chaput, P. Feneyrou, G. Berginc, O. Maury, C. Andraud, S. Parola, J. Mater. Chem. C (2014).
- [23] I. Levchuk, M. Sillanpää, C. Guillard, D. Gregori, D. Chateau, F. Chaput, F. Lerouge, S. Parola, J. Catal. 342 (2016) 117–124, <https://doi.org/10.1016/j.jcat.2016.07.015>.

- [24] D. Chateau, A. Liotta, F. Vadcard, J. Navarro, F. Chaput, J. Lermé, F. Lerouge, S. Parola, *Nanoscale*. 7 (2015) 1934–1943.
- [25] ASTM International, (2000), pp. 1–2, <https://doi.org/10.1520/D3363-00>.
- [26] M. Figueredo-Fernández, S. Gutiérrez-Alfaro, A. Acevedo-Merino, M.A. Manzano, *Sol. Energy* 158 (2017) 303–310, <https://doi.org/10.1016/j.solener.2017.09.006>.
- [27] A. APHA WPCF, (Ed), *Standard Methods for the Examination of Water and Wastewater*, 2008.
- [28] E. Nebot Sanz, I. Salcedo Dávila, J.A. Andrade Balao, J.M. Quiroga Alonso, *Water Res.* 41 (2007) 3141–3151, <https://doi.org/10.1016/j.watres.2007.04.008>.
- [29] J.D. Oliver, *FEMS Microbiol. Rev.* 34 (2010) 415–425.
- [30] K.G. Lindenaier, J.L. Darby, *Water Res.* 28 (1994) 805–817, [https://doi.org/10.1016/0043-1354\(94\)90087-6](https://doi.org/10.1016/0043-1354(94)90087-6).
- [31] M.A. Centeno, M.C. Hidalgo, M.I. Domínguez, J.A. Navio, J.A. Odriozola, *Catal. Lett.* 123 (2008) 198–206, <https://doi.org/10.1007/s10562-008-9448-y>.
- [32] M. Centeno, C. Portales, I. Carrizosa, J. Odriozola, *Catal. Lett.* 102 (2005) 289–297, <https://doi.org/10.1007/s10562-005-5871-5>.
- [33] Navio and Hidalgo, G. Colon, S.G. Botta, M.I. Litter, *Langmuir* 17 (2001) 202–210, <https://doi.org/10.1021/la000897d>.
- [34] I. Levchuk, M. Sillanpää, C. Guillard, D. Gregori, D. Chateau, F. Chaput, F. Lerouge, S. Parola, *J. Catal.* 342 (2016) 117–124, <https://doi.org/10.1016/j.jcat.2016.07.015>.
- [35] I. Levchuk, M. Sillanpää, C. Guillard, D. Gregori, D. Chateau, S. Parola, *Surf. Sci.* 383 (2016) 367–374, <https://doi.org/10.1016/j.apsusc.2016.04.008>.
- [36] J. Herrmann, J. Photochem. Photobiol. A 216 (2010) 85–93, <https://doi.org/10.1016/j.jphotochem.2010.05.015>.
- [37] B. Erdural, U. Bolukbasi, G. Karakas, J. Photochem. Photobiol. A Chem. 283 (2014) 29–37, <https://doi.org/10.1016/j.jphotochem.2014.03.016>.
- [38] A. Rincón, C. Pulgarin, *Appl. Catal. B* 49 (2004) 99–112, <https://doi.org/10.1016/j.apcatb.2003.11.013>.
- [39] R. van Grieken, J. Marugán, C. Pablos, L. Furones, A. López, *Appl. Catal. B* 100 (2010) 212–220, <https://doi.org/10.1016/j.apcatb.2010.07.034>.
- [40] A. Pal, S.O. Pehkonen, L.E. Yu, M.B. Ray, J. Photochem. Photobiol. A Chem. 186 (2007) 335–341, <https://doi.org/10.1016/j.jphotochem.2006.09.002>.
- [41] O.K. Dalrymple, E. Stefanakos, M.A. Trotz, D.Y. Goswami, *Appl. Catal. B* 98 (2010) 27–38, <https://doi.org/10.1016/j.apcatb.2010.05.001>.
- [42] Y. Chen, S. Yang, K. Wang, L. Lou, J. Photochem. Photobiol. A Chem. 172 (2005) 47–54, <https://doi.org/10.1016/j.jphotochem.2004.11.006>.
- [43] H. Son, S. Choi, E. Khan, K. Zoh, *Water Res.* 40 (2006) 692–698, <https://doi.org/10.1016/j.watres.2005.11.046>.
- [44] S. Nasser, A.H. Mahvi, M. Seyedsalehi, K. Yaghmaeian, R. Nabizadeh, M. Alimohammadi, G.H. Safari, *J. Mol. Liq.* 241 (2017) 704–714, <https://doi.org/10.1016/j.molliq.2017.05.137>.
- [45] P. Villegas-Guzman, J. Silva-Agredo, O. Florez, A.L. Giraldo-Aguirre, C. Pulgarin, R.A. Torres-Palma, *J. Environ. Manage.* 190 (2017) 72–79, <https://doi.org/10.1016/j.jenvman.2016.12.056>.
- [46] S. Giannakis, M.I.P. López, D. Spuhler, J.A.S. Pérez, P.F. Ibáñez, C. Pulgarin, *Appl. Catal. B* 199 (2016) 199–223.
- [47] L. Armelao, D. Barreca, G. Bottaro, A. Gasparotto, C. Maccato, C. Maragno, E. Tondello, U.L. Å tangar, M. Bergant, D. Mahne, *Nanotechnology* 18 (2007) 375709.
- [48] S. Rtimi, M. Pasqu, R. Sanjines, C. Pulgarin, M. Ben-Simon, A. Houas, J.-Lavanchy, J. Kiwi, *Appl. Catal. B* 138–139 (2013) 113–121, <https://doi.org/10.1016/j.apcatb.2013.01.066>.
- [49] T.P. Shareena Dasari, Y. Zhang, H. Yu, *Biochem. Pharmacol. (Los Angel)* 4 (2015) 199, <https://doi.org/10.4172/2167-0501.1000199>.
- [50] A. Furube, L. Du, K. Hara, R. Katoh, M. Tachiya, *J. Am. Chem. Soc.* 129 (2007) 14852–14853.